

- [16] Crystal data for (+)-1/urea (space group  $P3_112$ ):  $a = b = 8.1660(10)$ ,  $c = 55.2445(13)$  Å,  $V = 3190.8(1)$  Å<sup>3</sup> at 198 K;  $R_1 = 0.085$ ,  $wR_2 = 0.095$ , GOF 1.747 (based on  $F^2$ ), 5081 observed reflections with  $I \geq 2.00 \sigma(I)$ , 252 parameters, Flack  $x$  parameter (esd) =  $-1.38$  (1.66). Crystal data for (–)-1/urea (space group  $P3_212$ ):  $a = b = 8.1670(10)$ ,  $c = 55.2166(12)$  Å,  $V = 3189.5(1)$  Å<sup>3</sup> at 198 K;  $R_1 = 0.095$ ,  $wR_2 = 0.069$ , GOF 2.513 (all reflections, based on  $F^2$ ), 3670 observed reflections with  $I \geq 2.00 \sigma(I)$ , 252 parameters, Flack  $x$  parameter (esd) =  $-1.55$  (1.77). (Other trigonal UICs, such as 2,9-decanedione/urea<sup>[4]</sup> give similar results and errors. Extensive efforts to prepare heavy atom analogues amenable to Bijvoet analysis are underway.) CCDC-171162 ((–)-1/urea) and CCDC-171163 ((+)-1/urea) contain the supplementary crystallographic data for this paper. These data can be obtained free of charge via [www.ccdc.cam.ac.uk/conts/retrieving.html](http://www.ccdc.cam.ac.uk/conts/retrieving.html) (or from the Cambridge Crystallographic Data Centre, 12, Union Road, Cambridge CB21EZ, UK; fax: (+44)1223-336-033; or deposit@ccdc.cam.ac.uk).
- [17] U. Werner-Zwanziger, M. E. Brown, J. D. Chaney, E. J. Still, M. D. Hollingsworth, *Appl. Magn. Reson.* **1999**, *17*, 265–281.
- [18] M. D. Hollingsworth, U. Werner-Zwanziger, M. E. Brown, J. D. Chaney, J. C. Huffman, K. D. M. Harris, S. P. Smart, *J. Am. Chem. Soc.* **1999**, *121*, 9732–9733.
- [19] M. D. Hollingsworth, M. L. Peterson, K. L. Pate, B. D. Dinkelmeyer, M. E. Brown, *J. Am. Chem. Soc.* **2002**, *124*, in press.
- [20] W. Kaminsky, A. M. Glazer, *Z. Kristallogr.* **1997**, *212*, 283–296.
- [21] G. H. Posner, C. E. Whitten, P. E. McFarland, *J. Am. Chem. Soc.* **1972**, *94*, 5106–5108.

## Structural Analysis of C<sub>60</sub> Trimers by Direct Observation with Scanning Tunneling Microscopy \*\*

Masashi Kunitake,\* Shinobu Uemura, Osamu Ito, Koichi Fujiwara, Yasujiro Murata, and Koichi Komatsu\*

All-carbon fullerene oligomers and polymers have attracted considerable interest from a wide range of scientific and technological view points.<sup>[1]</sup> The formation, structure, and characteristics of fullerene oligomers, such as dimers and

trimers, and fullerene polymers are of particular interest because of their potential usefulness as molecular devices, and in the fields of optoelectronics and nanotechnology. These materials have been prepared under photochemical<sup>[2]</sup> or high-pressure/high-temperature conditions,<sup>[3]</sup> or by the action of alkali metals upon fullerenes.<sup>[4]</sup> Recently, it was found that the solid-state mechanochemical reaction of C<sub>60</sub> with potassium salts such as KCN, KOAc, and K<sub>2</sub>CO<sub>3</sub>, with highly reducing metals, or with solid aromatic amines under “high-speed vibration milling (HSVM)” conditions, can successfully produce the fullerene dimer, C<sub>120</sub>.<sup>[5, 6]</sup> Furthermore, the trimers (C<sub>180</sub>), which include a variety of structural isomers, were also found to be formed by this reaction.<sup>[7]</sup>

When C<sub>60</sub> was treated with 4-aminopyridine under HSVM conditions, analysis of the reaction mixture with high-pressure liquid chromatography (HPLC) using a Cosmosil 5PBB column and eluting with *o*-dichlorobenzene (*o*-DCB) showed two small peaks (fractions A and B) corresponding to the trimer (C<sub>180</sub>). These peaks appeared after the major peaks for C<sub>60</sub> and the dimer (C<sub>120</sub>). Upon evaporation of the solvent, the material giving rise to the C<sub>180</sub> peaks amounted to 4 % yield based on C<sub>60</sub>. Further analysis and separation using different HPLC conditions with a Cosmosil Buckyprep column and eluting with toluene revealed that fraction A consisted of at least three isomers (A1, A2,<sup>[16]</sup> and A3), while fraction B was a single component (Figure 1). The identity of C<sub>180</sub> was estab-

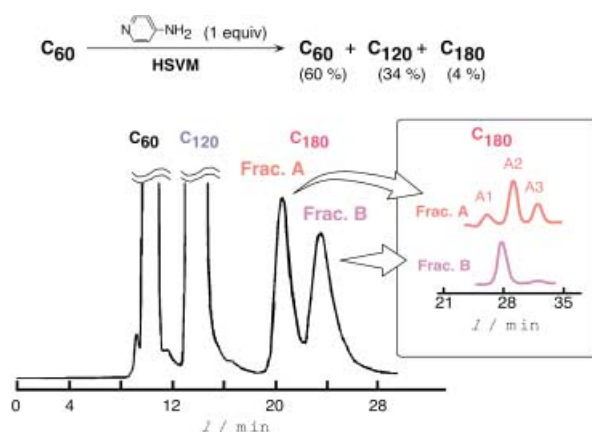


Figure 1. Elution traces for HPLC separation of C<sub>180</sub> isomers, with UV detection at 326 nm. Left: Cosmosil 5PBB column eluting with *o*-DCB, and right (inset): Cosmosil Buckyprep column eluting with toluene.

lished by solution-phase cyanation and observation of the peak arising from the C<sub>180</sub>(CN)<sup>–</sup> ion by atmospheric pressure chemical ionization (APCI) mass spectral analysis (negative ion mode). APCI mass analysis of the C<sub>180</sub> itself exhibited only the fragment peak of C<sub>60</sub>.<sup>[7]</sup>

Unfortunately, the extremely low solubility of C<sub>180</sub> in ordinary solvents did not allow the chemical structure to be determined by <sup>13</sup>C NMR spectroscopy. Such low solubility also made it difficult to prepare single-crystal samples of C<sub>180</sub> for X-ray diffraction analysis. In the present study, however, we successfully achieved structural identifications of the C<sub>180</sub> isomers by direct visualization using scanning tunneling microscopy (STM).

[\*] Prof. Dr. M. Kunitake, Dr. S. Uemura  
Department of Applied Chemistry & Biochemistry  
Faculty of Engineering, Kumamoto University  
Kurokami, Kumamoto 860-8555 (Japan)  
Fax: (+81)96-342-3673  
E-mail: kunitake@chem.kumamoto-u.ac.jp

Prof. Dr. K. Komatsu, K. Fujiwara, Dr. Y. Murata  
Institute for Chemical Research  
Kyoto University  
Uji, Kyoto 611-0011 (Japan)  
Fax: (+81)774-38-3178  
E-mail: komatsu@scl.kyoto-u.ac.jp

Prof. Dr. O. Ito  
Institute of Multidisciplinary Research for Advanced Materials  
Tohoku University, Katahira, Sendai, 980-8577 (Japan)

[\*\*] This work was supported in part by Grants-in-Aids for Scientific Research from the Ministry of Education, Culture, Sports, Science, and Technology, Japan and the CREST-JST, Japan.

Molecular imaging of pure  $C_{60}$  and its derivatives by STM has been reported.<sup>[8–15]</sup> In general, the STM observations of fullerenes were conducted in an ultrahigh-vacuum (UHV) environment by using epitaxial adlayers prepared by sublimation. The sublimation technique, however, can not be applied to the preparation of  $C_{180}$  films, because of the ready thermal decomposition of  $C_{180}$  to  $C_{60}$ , as observed in the mass spectral analysis (APCI). Recently, we found a simple preparation for, and in situ STM observation of, fullerene epitaxial adlayers, based on a “wet process” in which the measurements were conducted under ambient conditions.<sup>[14, 15]</sup> The simple transfer of Langmuir films at the air–water interface allowed us to prepare epitaxial adlayers of fullerenes on Au(111) surfaces. The formed epitaxial adlayers of  $C_{60}$  and  $C_{60}/C_{70}$  were found to be essentially the same as those prepared by sublimation in UHV.<sup>[14, 15]</sup> Therefore, we attempted the application of this technique to the preparation of the  $C_{180}$  adlayers for STM imaging.

The Langmuir films of each of the fractions A, A2, and B of the  $C_{180}$  isomers at the air–water interface were transferred onto an intact Au(111) surface in a single step by passing the Au(111) surface through the air–water interface.<sup>[14]</sup> As in the case of dimer  $C_{120}$ ,  $\pi$ -A isotherms of  $C_{180}$  revealed only small surface pressures of less than several  $\text{nm}^2\text{m}^{-1}$ . Because of the lack of amphiphilicity, it seemed impossible to form an ideal monolayer of  $C_{180}$ . In this technique, the Langmuir films were used only to introduce materials at the monolayer level. After the transfer, the sample was placed in an electrochemical STM cell filled with 0.1M perchloric acid. The details of sample preparation and the in situ STM observation technique have been described.<sup>[14, 15]</sup> The combination of the wet-process preparation using transfer of Langmuir films to Au(111) with in situ STM observation is advantageous, since a more uniform sample surface is obtained than that given by the casting of  $C_{180}$  from the organic solution and STM observation under air.

The surface morphologies of  $C_{180}$  adlayers were completely different from those of  $C_{60}$ . Figure 2 shows typical STM images of the  $C_{180}$  adlayers (fraction A2 and fraction B) and  $C_{60}$  adlayer on Au(111) surfaces. As mentioned above, the image of  $C_{60}$  revealed ordered molecular adlayers with hexagonal packing, although the films had many disordered regions (Figure 2C). In contrast, the  $C_{180}$  fractions (Figure 2A and B) gave entirely disordered adlayers and no ordered region was observed. The disordered adlayers are probably caused by a stronger interac-

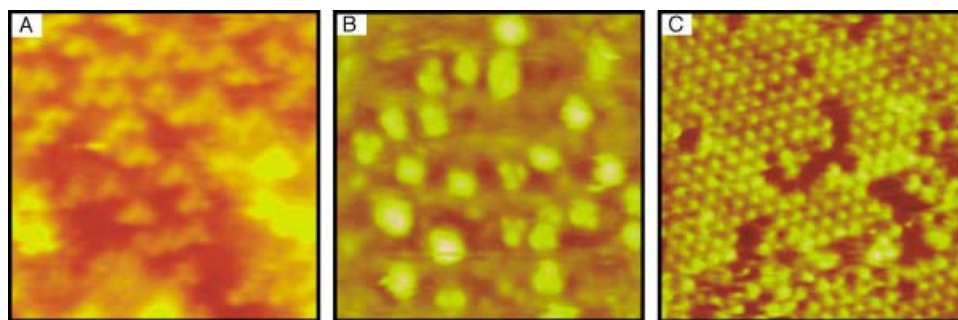


Figure 2. Typical in situ STM images for fraction A2 (A;  $16.5 \times 16.5 \text{ nm}^2$ ) and fraction B (B;  $12.2 \times 12.2 \text{ nm}^2$ ) of randomly adsorbed  $C_{180}$  adlayers and of a  $C_{60}$  epitaxial adlayer (C;  $18.2 \times 18.2 \text{ nm}^2$ ) on Au(111) surfaces. Images A and B were collected with  $E_s = 0.36$  and  $0.38 \text{ V}$ ,  $E_{\text{tip}} = -0.40$  and  $-0.41 \text{ V}$  versus saturated calomel electrode (SCE), and  $I_t = 0.38$  and  $0.9 \text{ nA}$ , respectively. Image C was collected with  $E_s = 0.10 \text{ V}$ ,  $E_{\text{tip}} = -0.05 \text{ V}$ , and  $I_t = 1.0 \text{ nA}$ . There is no significant influence of sample potentials upon the observed images.

tion between  $C_{180}$  and the substrate (Au(111)). Submolecular high-resolution STM images are expected to reveal the structural differences among the  $C_{180}$  isomers. The disordered adlayer may facilitate the recognition of the isolated  $C_{180}$  isomers, which appear as several distinct structures lying flat on the surface. These structures consist of three bright spots, which correspond to each of the  $C_{60}$  moieties of  $C_{180}$ . The shape of  $C_{180}$  in fraction B appears quite different from that in fraction A2 (Figure 2).

Fraction B (Figure 2B) was expected to contain an isomer with significantly different structural characteristics from other isomers, because it gave a single peak under the two different HPLC conditions (Figure 1). Bright spots arranged in a triangular shape can be clearly recognized in Figure 2B.

Figure 3 shows typical high-resolution STM images of the  $C_{180}$  isomer in fraction B. It was found to have a cyclic triangular shape. The triangular shape with high symmetry is clearly attributable to the flat-lying “*cis-2/cis-2/cis-2*” isomer. The observed distance between spots in the cyclic feature is  $0.7\text{--}0.8 \text{ nm}$ , which is obviously smaller than the intermolecular distance,  $1.0 \text{ nm}$ , observed in the  $C_{60}$  epitaxial lattice. Thus the possibility of an accidental triangular assembly of three  $C_{60}$  molecules on Au(111) lattices is clearly ruled out. No other image, which could be attributed to other isomers, was observed in fraction B.

Ab initio molecular orbital calculations of the total electron energy ( $\Delta E_{\text{tot}}$ ) using HF/3-21G afford information about the

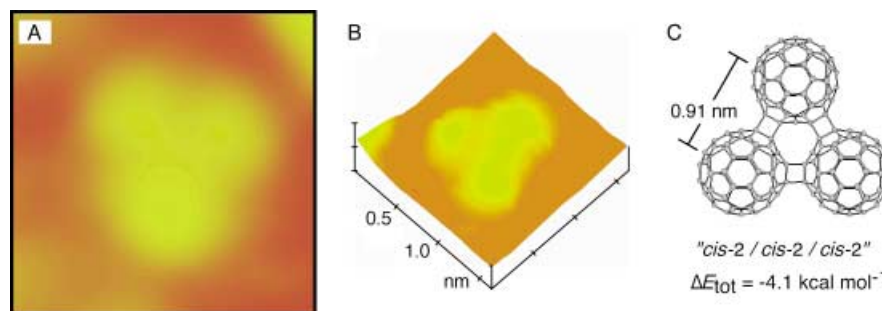


Figure 3. Typical high-resolution STM images of a  $C_{180}$  molecule on Au(111) surfaces prepared from fraction B, A) top view,  $1.67 \times 1.67 \text{ nm}^2$ , B) surface plot, and C) the chemical structure of the cyclic “*cis-2/cis-2/cis-2*” isomer. The image was collected with  $E_s = 0.38 \text{ V}$ ,  $E_{\text{tip}} = -0.41 \text{ V}$ , and  $I_t = 0.9 \text{ nA}$ .

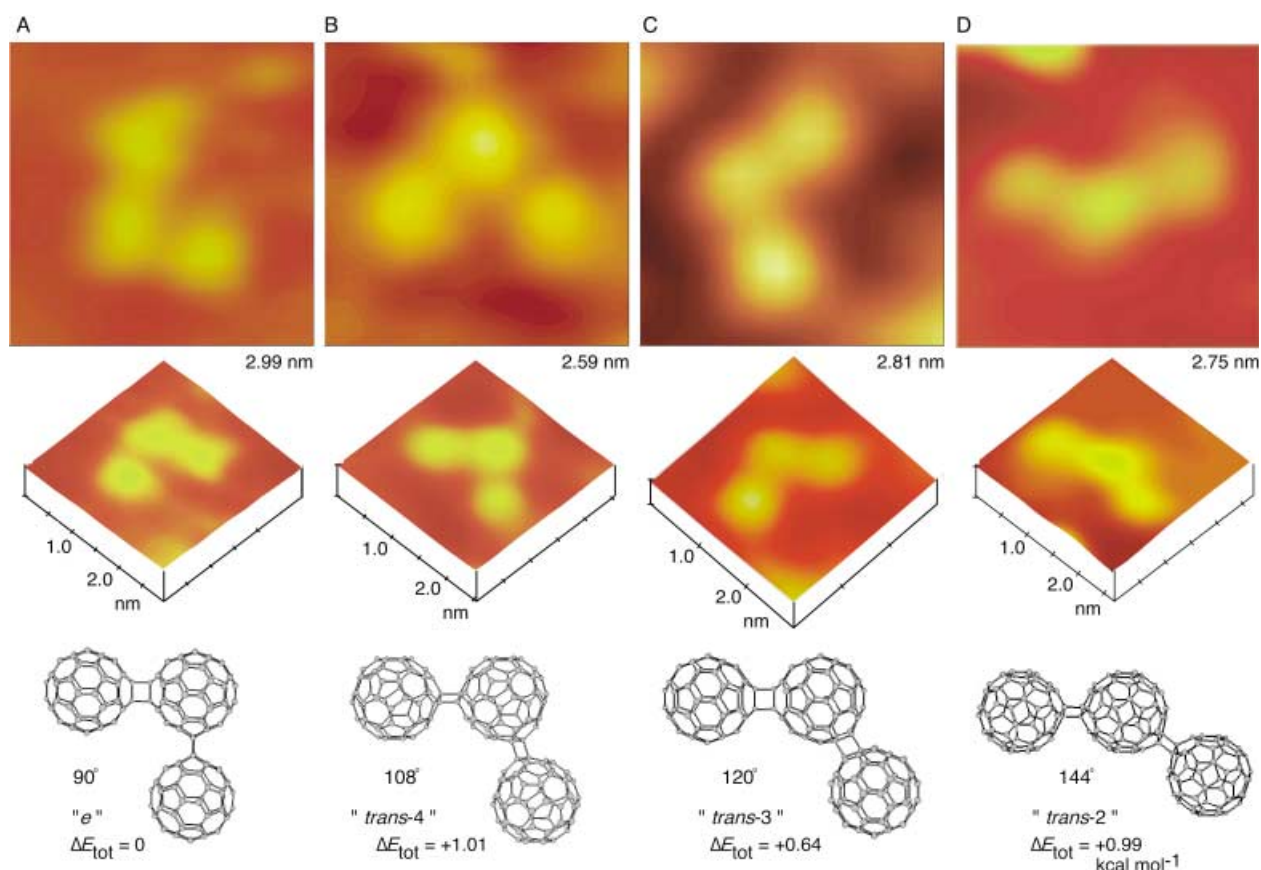


Figure 4. A variety of high-resolution STM images (top view and surface plot, below) of  $C_{180}$  molecules obtained from fraction A, and the chemical structures of the corresponding isomers. The images were collected with  $E_s = 0.36$  V and  $E_{tip} = -0.28$  V.

relative stabilities of the  $C_{180}$  isomers. Of the expected isomers, which include noncyclic isomers, the “*cis-2/cis-2/cis-2*” isomer was found to be the most stable ( $-4.1$  kcal mol $^{-1}$  relative to the “*e*” isomer; Figure 4). STM images obtained from fraction A exhibited mixed structures consisting of four isomers, which possessed “noncyclic extended” structures (Figure 4). Each  $C_{180}$  molecule in the STM images appears as three spots connected at specific angles. The observed fold angles were approximately 90, 108, 120, and 144°, which can be attributed to “*e*”, “*trans-4*”, “*trans-3*”, and “*trans-2*” isomers, respectively. Neither the cyclic “*cis-2/cis-2/cis-2*” isomer nor the noncyclic “*cis*” isomers with a fold angle of less than 90° were observed.

The ratio of isomer content in fraction A was roughly estimated by counting the observed shapes of more than 100 molecular features in STM images. This surface content ratio should approximately reflect the content of each isomer in the whole of fraction A. The content ratios for “*e*”, “*trans-4*”, “*trans-3*”, and “*trans-2*” isomers were found to be 58, 25, 13, and 4%, respectively.

In addition, the STM image of fraction A2, which gave the largest analytical HPLC peak among the peaks in fraction A and was successfully isolated, indicated that this fraction is composed of only the “*e*” isomer of  $C_{180}$ . This result is in agreement not only with the isomer content in fraction A but also with molecular orbital calculations which predict the highest stability for this isomer of all the isomers with extended structures. The  $\Delta E_{tot}$  values calculated by HF/3-

21G for “*trans-4*”, “*trans-3*”, “*trans-2*”, and “*trans-1*” isomers were +1.01, +0.64, +0.99, and +0.90 kcal mol $^{-1}$  relative to the “*e*” isomer, respectively. On the other hand, the small difference in the calculated  $\Delta E_{tot}$  values among the isomers is reflected in the observation of STM images, which indicated that several isomers are simultaneously produced by the HSVM treatment of  $C_{60}$ . Interestingly, the “*trans-1*” isomer was hardly observed in fraction A. Statistically, the possibility that  $C_{60}$  will react at the “*trans-1*” position of  $C_{120}$  is 1/4 of the possibility of reaction at other positions of  $C_{120}$ , which gives the “folded” isomers. This low probability may be one of the reasons for the absence of the “*trans-1*” isomer.

In conclusion, we succeeded in the direct observation of thermally and photochemically labile  $C_{180}$  isomers by the transfer of Langmuir films onto Au(111) surfaces. The components of HPLC A and B peaks were clearly identified. The content ratio of the isomers was also determined by STM observation, which was in good agreement with the  $\Delta E_{tot}$  values obtained by molecular orbital calculations. Thus, STM has, for the first time, been successfully applied to identify the isomeric structures of  $C_{60}$  trimers, which are difficult to determine spectroscopically, as a result of their extremely low solubility.

Examination of the unique electronic and spectroscopic characteristics of these  $C_{180}$  isomers<sup>[17]</sup> is in progress to put them to use in electronic and photonic devices.

Received: October 23, 2001 [Z18109]



- [1] a) *Fullerene Polymers and Fullerene Polymer Composites* (Eds.: P. C. Eklund, A. M. Rao), Springer, Berlin, **2000**; b) *The Chemistry of Fullerenes* (Ed.: R. Taylor), World Scientific, Singapore, **1995**.
- [2] A. M. Rao, P. Zhou, K.-A. Wang, G. T. Hager, J. M. Holden, Y. Wang, W.-T. Lee, X.-X. Bi, P. C. Eklund, D. S. Cornett, M. A. Duncan, I. J. Amster, *Science* **1993**, 259, 955–957.
- [3] Y. Iwasa, T. Arima, R. M. Fleming, T. Siegrist, O. Zhou, R. C. Haddon, L. J. Rothberg, K. B. Lyons, H. L. Carter Jr., A. F. Hebard, R. Tycko, G. Dabbagh, J. J. Krajewski, G. A. Thomas, T. Yagi, *Science* **1994**, 264, 1570–1572.
- [4] S. Pekker, A. Janossy, L. Mihaly, O. Chauvet, M. Carrard, L. Forro, *Science* **1994**, 265, 1077–1078.
- [5] G.-W. Wang, K. Komatsu, Y. Murata, M. Shiro, *Nature* **1997**, 387, 583–586.
- [6] K. Komatsu, G.-W. Wang, Y. Murata, T. Tanaka, K. Fujiwara, K. Yamamoto, M. Saunders, *J. Org. Chem.* **1998**, 63, 9358–9366.
- [7] K. Komatsu, K. Fujiwara, Y. Murata, *Chem. Lett.* **2000**, 1016–1017.
- [8] R. J. Wilson, G. Meijer, D. S. Bethune, R. D. Johnson, D. D. Chambliss, M. S. De Vries, H. E. Hunziker, H. R. Wendt, *Nature* **1990**, 348, 621–622.
- [9] C. Jehoulet, Y. S. Obeng, Y.-T. Kim, F. Zhou, A. J. Bard, *J. Am. Chem. Soc.* **1992**, 114, 4237–4247.
- [10] Y. Zhang, X. Gao, M. J. Weaver, *J. Phys. Chem.* **1992**, 96, 510–513.
- [11] T. Sakurai, X.-D. Wang, Q. K. Xue, Y. Hasegawa, T. Hashizume, H. Shinohara, *Prog. Surf. Sci.* **1996**, 51, 263–408.
- [12] J. W. G. Wildoer, L. C. Venema, A. G. Rinzier, R. E. Smalley, E. Richard, C. Dekker, *Nature* **1998**, 391, 59–62.
- [13] T. W. Odom, J.-L. Huang, P. Kim, C. M. Lieber, *Nature* **1998**, 391, 62–64.
- [14] S. Uemura, M. Sakata, M. Kunitake, I. Taniguchi, C. Hirayama, *Chem. Lett.* **1999**, 536–537.
- [15] S. Uemura, M. Sakata, M. Kunitake, I. Taniguchi, C. Hirayama, *Langmuir* **2001**, 17, 5–7.
- [16] Of the components in fraction A, only the major component, fraction A2, was successfully separated from fraction A by carefully repeated HPLC.
- [17] M. Fujitsuka, K. Fujiwara, Y. Murata, S. Uemura, M. Kunitake, O. Ito, K. Komatsu, *Chem. Lett.* **2001**, 384–385.

## Computational Prediction of the Phase Transformation of Two As-Synthesized Oxyfluorinated Compounds into the Zeotype CHA Forms

Stéphanie Girard, Alain Tuel, Caroline Mellot-Draznieks, and Gérard Férey\*

The numerous syntheses of templated inorganic open frameworks in hydrothermal conditions<sup>[1]</sup> were the starting point for the development of porous solids obtained by calcination, with applications as molecular sieves, for adsorption or catalytic purposes. Indeed the structure-directing agents, used during the synthesis of such compounds, are often incorporated in the final structure. Upon thermal treatment

(calcination), these template molecules can usually be removed, along with other species, such as water molecules and hydroxy groups. However, whereas the crystal structures of as-synthesized solids are well characterized, those of calcined solids, which are of crucial interest, are scarcely described, this is because of their powder form and a result of the difficulties of ab initio resolution from powder data.

Fortunately, in the last ten years, computational tools have proved their efficiency for simulating the structures and energetics of inorganic solids.<sup>[2]</sup> Recently, we have successfully investigated the dehydroxylation process and organic-template extraction of two as-synthesized aluminophosphates, namely AlPO<sub>4</sub>-14,<sup>[3]</sup> and MIL-34.<sup>[4]</sup> Starting from the knowledge of the as-synthesized structure only, all the atoms that are known to be eliminated upon calcination are removed. The so-modified AlPO<sub>4</sub>-14 and MIL-34 model frameworks were then submitted to energy minimizations. This way, we predicted the calcined AlPO<sub>4</sub>-14 structure in excellent agreement with the experimentally calcined AlPO<sub>4</sub>-14,<sup>[3]</sup> which had already been obtained before our calculations. Above all, we successfully anticipated the structures and energetics of the calcined form of MIL-34, before it was actually experimentally calcined. The cell parameters and atomic coordinates predicted from the simulation were used to perform the Rietveld refinement of the calcined sample powder pattern. The present work aims at developing a computational approach of the calcination process of fluorinated templated structures.

Indeed, fluoride ions can belong to the framework or act as template. In the continuously expanding number of synthetic oxyfluorinated AlPOs<sup>[5,6]</sup> and GaPOs, which include three-dimensional (3D) frameworks with very large pores such as cloverite<sup>[7]</sup> or MIL-31,<sup>[8]</sup> fluoride ions may occupy one or two vertices of the Al/Ga polyhedra in terminal or bridging positions, such as in ULM-6<sup>[5]</sup> or CJ2<sup>[5]</sup> respectively, or act as anionic template, such as in cloverite,<sup>[7]</sup> GaPO<sub>4</sub>-LTA,<sup>[9]</sup> and ULM-18,<sup>[10]</sup> where they are encapsulated in D4R cages (Figure 1).

Regarding calcination, fluorine anions are deemed to play a specific role in the stabilization of the as-synthesized structure. This function is strongly related to their position in the framework and their high electronegativity, which often leads to strong hydrogen bonding and therefore a tighter amine–framework interaction. However, the mechanisms involved at the atomic scale during the calcination process are complex and still not clearly elucidated.

Here, we present the first attempt to use a computational approach to study the structural evolution during the dehydrofluorination process and template extraction of two isotopic as-synthesized oxyfluorinated open-framework structures, an aluminophosphate UT-6, (Al<sub>6</sub>P<sub>6</sub>O<sub>24</sub>F<sub>2</sub>)-(C<sub>5</sub>H<sub>5</sub>NH)<sub>2</sub>-(H<sub>2</sub>O)<sub>0.3</sub>,<sup>[6]</sup> and a gallophosphate GaPO-tricl.CHA, (Ga<sub>6</sub>P<sub>6</sub>O<sub>24</sub>F<sub>2</sub>)-(C<sub>4</sub>N<sub>2</sub>H<sub>6</sub>)<sub>2</sub>-(H<sub>2</sub>O).<sup>[11]</sup> As shown from their X-ray diffraction (XRD) patterns, both structures adopt upon calcination the CHA zeotype,<sup>[12]</sup> which correspond to the chabazite structure.

Herein, the experimental structures of the as-synthesized UT-6 and GaPO-tricl.CHA were taken as starting points for our simulations. UT-6 and GaPO-tricl.CHA are isostructural

[\*] Prof. G. Férey, Dr. S. Girard, Dr. C. Mellot-Draznieks  
 Institut Lavoisier, UMR CNRS 8637  
 Université de Versailles Saint-Quentin  
 45, Avenue des Etats-Unis, 78035 Versailles Cedex (France)  
 Fax: (+33) 1-3925-4358  
 E-mail: ferey@chimie.uvsq.fr  
 Dr. A. Tuel  
 Institut de Recherches sur la Catalyse, C.N.R.S.  
 2 avenue Albert Einstein, 69626 Villeurbanne Cedex (France)